

Automated Diagnostic System for Laryngeal Hemiplegia Using Endoscopic Image

Md. Musfequs Salehin, Lihong Zheng, and Junbin Gao
School of Computing & Mathematics, Charles Sturt University, Australia
Email: {msalehin, lzheng, jbgao}@csu.edu.au

Abstract—Laryngeal hemiplegia is a naturally occurring disease of a horse recognized as a common reason of the poor performance. This syndrome is diagnosed by a human through an endoscopic observation. The asymmetry of arytenoid cartilages is calculated by left to right angle quotients (LRQ). However, human inspection may misdiagnose the disease. Therefore, an automatic diagnostic system is expected to analysis the asymmetric view of laryngeal hemiplegia. In this paper, we have proposed an automatic way to analysis laryngeal hemiplegia by combining image segmentation and parabola fitting algorithms. Our method includes six steps: (1) hierarchical contour map is achieved by a state-of-the-art hierarchical image segmentation method joining Global Probability of Boundary (gPb), Oriented Watershed Transform (OWT), and Ultrametric Contour Map (UCM); (2) key curves are extracted; (3) boundaries are confirmed by Parabola fitting method; (4) dorsal-most point of rima glottidis is selected; (5) proximal-most point is identified and (6) LRQ is calculated as the final measurement. To evaluate the accuracy of our proposed method, a dataset of horse larynx endoscopic images has been built up and tested. Experimental results have shown that the proposed method has good performance.

Index Terms—horse larynx, endoscopic image, hierarchical segmentation, corner detection, LRQ calculation

I. INTRODUCTION

Laryngeal hemiplegia (one-sided paralysis) is the most common cause of horses making abnormal respiratory noises during inspiration at fast exercise. The noise is caused by partial or total paralysis of horse larynx [1]. An example of laryngeal paralysis is the case like that either side of arytenoid is hanging down into the airway. Frequently this is caused by damage to the left recurrent laryngeal nerve. It can also be related to damage to the arytenoid itself such as infection of the cartilage. It has been noted that almost 42% of Draught horses [2] and 1.8-10.7% of Thoroughbred racehorses [3] have high prevalence for this disease. This idiopathic disorder affects the left laryngeal nerve and causes neurogenic atrophy of the left cricoarytenoid dorsalis (CAD) muscle which works as a primary abductor of the arytenoid cartilages [1]. Due to the loss of left arytenoid cartilage

abduction, the cross sectional area of the rima glottis is decreased.

Through endoscopic examination, i.e. a flexible periscope-type instrument is passed through the nose, into the pharynx, to look at the larynx as the horse breaths. Both sides of the larynx should open and close in synchrony, almost symmetrically and completely. However, the left side of the larynx of a horse affected by laryngeal hemiplegia moves sluggishly and incompletely, 'hanging' into the larynx and obstructing airflow during inspiration [4]. In moderately severe cases, it may help to do a 'Hobday' operation in which a piece of laryngeal tissue is surgically removed to encourage a scar to form to 'tighten' the larynx in a more open position. In more severe cases, a 'tie-back' operation is often recommended. This more elaborate operation places sutures in the paralysed side to pull and hold it open.

By watching the endoscope screen, the clinics may do two types of assessments. One is to check right to left angle quotients (LRQ) and another one is to verify glottis cross-sectional area ratios (CSAR) as reported in [5]. LRQ method is more suitable for diagnosis of laryngeal hemiplegia compared to CSAR [6]. However until today, LRQ process is done manually. It is perceptible that human measurement is time consuming and may generate inaccurate and inconsistent result which may mislead to make clinical decision, vetting procedure and disease diagnosis.

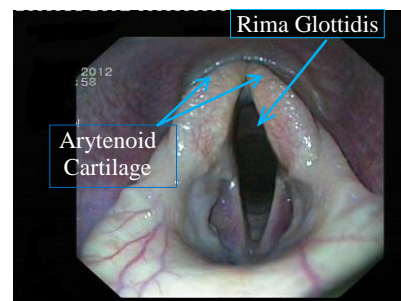


Figure 1. One sample of endoscopic image of horse larynx

Again, examinations done by one or many observers on an individual horse would probably vary in results. In this paper, we have proposed a method to measure LRQ from horse larynx endoscopic image automatically and accurately. Through experiment on a new dataset of horse larynx endoscopic images, we have shown effectiveness of our proposed method in terms of accuracy.

The organization of this paper is as follows: Section II briefly describes the literature review; the proposed method is described in Section III; Section IV presents the results and discussion and lastly, we conclude the paper in Section V.

II. A BRIEF REVIEW OF THE PREVIOUS RESEARCH

Computer-aided diagnosis is an important application of biomedical imaging. Its main purpose is to assist a doctor in making diagnostic decision. To achieve this goal, accurate segmentation of medical images is very crucial. Histogram thresholding [7], region growing method [8] and edge detection [9]-[12] are the most conventional approaches for image segmentation. Histogram thresholding utilizes global information of color distribution to segment images. The technique works well in gray image while it also shows poor performance for color images. The region growing methods segment image based on local information. However, success of the technique depends on initial seeds and it is difficult to define the terminating condition for this approach. For detecting edge, Roberts [9], Sobel [10] and Prewitt [11] used convolution of local derivative filters in gray image. The Canny detector [12] extracts edge by non-maximum suppression and hysteresis thresholding steps. Edge based segmentation method, on the other hand, often produces no connected boundaries and detects false edge points.

The most widely used segmentation approaches are based on combination of local brightness, colour and texture and grouping of these features by fitting mixture models [13], mode-finding [14] and graph partitioning [15]. Felzenszwalb and Huttenlocher [15] developed a graph-based region merging algorithm for separating image pixels into component. Here nodes are represented by pixels and the edge weights are defined by dissimilarity measurements among nodes. A different clustering framework has been introduced in the Mean Shift algorithm [14]. Both spatial coordinate and colour values are used to represent pixels in the joint spatial-range domain. A convergence point for each pixel is calculated by implementing mean shift filtering. Based on bandwidth parameters of this convergence points, regions are formed.

Recently, a state-of-the-art algorithm gPb-OWT-UCM for contour detection and image segmentation is proposed [16]. Multiple low-level cues, such as, brightness, color and texture are combined with the global information to detect the contour in gPb (global probability of boundary) which is better than other detectors such as canny detector [12]. A two-step generic grouping algorithm is used to produce high-quality image segmentation from these detected contours. The first step is a newly proposed Oriented Watershed Transform (OWT) [16] to build the initial closed region sets from the contour. This reweighting process (OWT) involves estimating an orientation on each arc pixel, assigning boundary strength to each pixel on an arc using the oriented contour detector and allocating average boundary strength to all pixels on the arc. In second step, an accumulated clustering procedure is used to form a hierarchy represented by

Ultrametric Contour Map (UCM) [16] from these regions. The greedy-graph based region merging algorithm is used to take regions, arcs and weights assigned by OWT as input and to produce a region tree as the result where the root is the real-valued image and leaves are tiered regions. The algorithm sorts the similar arcs and combines the most similar region repetitively. As only the higher weighted contours are considered during merging process at each step of the algorithm, region tree has an indexed hierarchy structure. For this reason, UCM can be used to represent the hierarchy of regions. By construction, UCM has the ability to yield a set of closed contours for any threshold value. The other reasons of using OWT and UCM in this research are that it has no parameter to tune and it is tested on every data set and for every benchmark.

III. OUR APPROACH

Due to the structure of horse larynx, the proposed automatic diagnostic method has six steps. The details are presented in this section as follows.

A. Endoscopic Image Segmentation

In this proposed scheme, we have used state-of-the-art gPb-OWT-UCM algorithm [16] to detect contour and segment endoscopic image (Fig. 2(a)). This method uses gPb to identify contour of an object. After implementing gPb, the obtained contours of larynx are shown in Fig. 2(b). The second part of the segmentation method (OWT) is used to form closed regions from the contours detected by gPb. Fig. 2(c) shows the closed regions. After that, a hierarchical region tree is formed by using UCM and the result is shown in Fig. 2(d).

B. Key Curves Extraction

After image segmentation, rich edge information has been found from UCM result (see Fig. 2 (d)). Two key curves which help the calculation of LRQ need to be extracted from the edge map. One of the properties of UCM is that it assigns average boundary strength to all pixels on the contour. We have used this unique value to extract key curves. In addition, shape, length and position of contour are used as the selective criteria.

Firstly, we have made the first list containing values for contours used in UCM and sorted in descending order. Then a value from the first list is selected and contours containing that value are highlighted. After that, the values, lengths and positions of the contours are saved in the second list. This process is used for each value in the first list. So, the second list includes information about the value, length and position of each contour.

It is observed that the first row of the second sorted list which contains the longest contours represents endoscopy image boundary, the second and the third rows present boundaries of arytenoid cartilages and rima glottidis respectively. Two separate images are generated for arytenoid cartilages (AC) (Fig. 2(e)) and rima glottidis (RG) (Fig. 2(f)) using the values assigned by UCM and

pixel positions of the boundary saved in second and third row of the second sorted list.

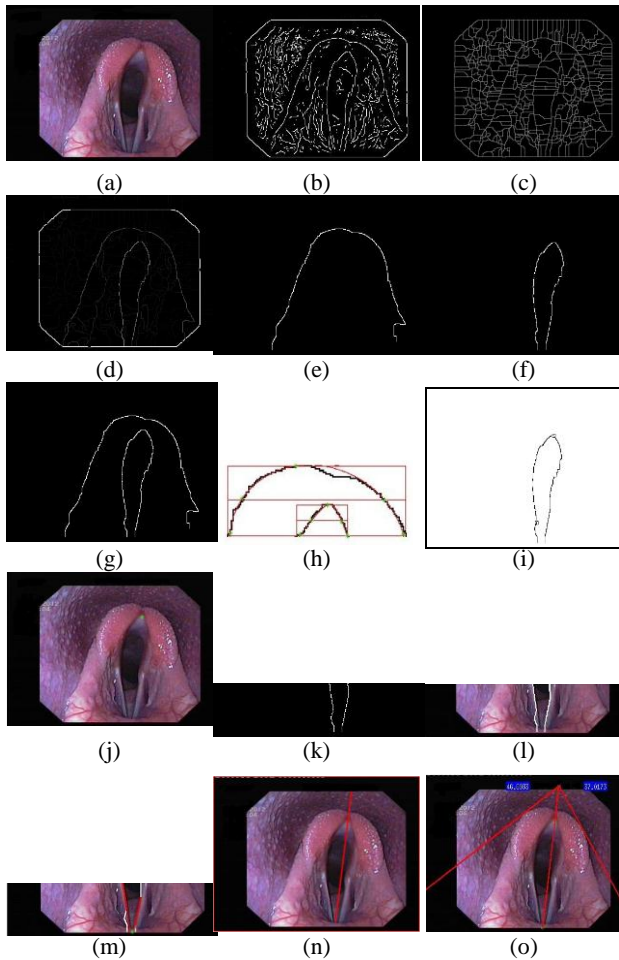


Figure 2. The processing sequence of an endoscopic image by our proposed method to measure LRQ

C. Parabola Fitting for Boundary Confirmation

Obviously, the shape of AC and RG are similar to parabola. To confirm detection of the boundaries of AC and RG from the endoscopic image of horse larynx after the extraction of the two key curves from UCM in the previous step, parabola fitting method is applied here to verify the two key curves. At first, the images of AC and RG are merged in a one image (see Fig. 2(g)). Following that, the merged image is cropped (shown in Fig. 2(h)) by the upper point obtained from the highest point from the curve of AC, the lower point achieved from 20 pixels below the highest point from the curve of RG and the left and right point from the first non zero pixel of both left and right side of the image. In the next step, a bounding box is built up for each curve within the cropped image. As shown in Fig. 3, five points are selected to draw a parabola as expected.

The top most point of the curve touching the upper line of the bounding box is selected as first point (P1). The second (P2) and third (P3) points are picked from one pixel above and below of the intersecting points of the curve and the midline of the bounding box. The ending points of the curve that are on the lower line and one

point above of the lower line of the box are chosen as fourth (P4) and fifth points (P5). Therefore, a parabola can be drawn using these five points by Pascal's theorem [17]. According to the theorem, when a hexagon is marked in a parabola, three intersecting points are got by connecting three pairs of opposite lines of hexagon excepting parallel case. These three points have the property of collinearity. Parabola follows this property. To avoid exception case of Pascal's theorem, two points are not selected from the same line of the bounding box. Five points of the hexagon are selected from the curve and the locus of sixth point is the entire parabola.

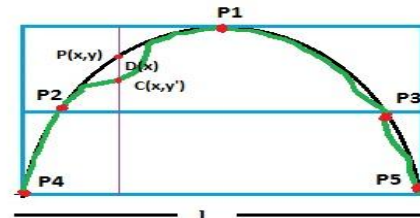


Figure 3. Bounding box to extract five points (P1-P5).

The vertical distance $D(x)$ between an actual point of the curve $C(x, y')$ and ideal point of the drawn parabola $P(x, y)$ (Fig. 3) is measured in each point of the bounding box using (1).

$$D(x) = ||P(x, y) - C(x, y')|| \quad (1)$$

Then the average difference of the vertical distances is calculated using (2).

$$D_{avg} = \frac{\sum_{x=1}^l D(x)}{l} \quad (2)$$

Here, l is the length of the bounding box. If D_{avg} is less than a threshold (T), it is confirmed that target boundary is selected. This process is performed for two curves. The threshold value 10 is selected for both cases. If any curve does not satisfy this condition, a new curve is selected from the second sorted list.

D. Dorsal-Most Point of Rima Glottidis Detection

To detect the dorsal point of rima glottidis, a corner detection method named Chord to Point Angle Accumulation (CPAA) [18] is used to RG image got from Section III.B. This corner detection method uses two chords and an angle between these chords to identify corners in a curve. As a result, it can detect multiple nearer corners. Again, only angle threshold ($\alpha_{Th} = 150^\circ$) is used for the refinement process in this approach. More importantly, it does not need any more parameters to tune. For all these reasons, CPAA is applied to detect corners in this method. After detecting corners (Fig. 2(i)), the top most corner is selected as the dorsal point of rima glottidis (Fig. 2(j)).

E. Proximal-Most Point of Rima Glottidis Detection

Sometimes the lower part of the curves in RG image is open and the shapes are very complicated. Five steps are used to detect the proximal-most point of the RG

image. Firstly, one-third of lower part of RG image is cropped (Fig. 2(k)); then line segmentation method [19] is implemented to get the smooth edge from complex shaped RG (Fig. 2(l)); after that, a horizontal line is drawn to connect the lowest point of the curve; next, two longest segmented lines that can be used to form an angle with its vertex on or below the horizontal line are selected and extended up to the horizontal line; lastly, the midpoint of the intersection points of the extended lines and horizontal line is identified as the proximal – most point of RG image (Fig. 2(m)).

F. LRQ Calculation

To measure LRQ, we have followed the conventional method proposed by Herholz and Straub [20]. The dorsal-most and proximal-most point are plotted in endoscopic image and these two points are connected to get the vertical line as the symmetrical axis (Fig. 2(n)). The vertical line is then extended to one-third of length between of the two points mentioned above. From this top point of the extended line, two tangent lines are drawn on both left and right arytenoid cartilage. Later, the angle (AL) between vertical line and left tangent line and the angle (AR) between vertical line and right tangent line are calculated. By dividing AR by AL, the value of LRQ is figured out (Fig. 2(o)) which indicates the degree of the left arytenoid abduction. LRQ is defined as

$$LRQ = \frac{AR}{AL} \tag{3}$$

IV. RESULTS AND DISCUSSION

The database of endoscopic images of horse larynx is built up from the images obtained from the Veterinary Clinical Centre, Charles Sturt University, Australia. Our proposed method was tested and evaluated on the images in the database. To the best of our knowledge, there is no such dataset in the literature. To assess the accuracy of the introduced approach, we used traditional manual calculation of LRQ as a ground truth. The output samples of the proposed scheme which can be used to evaluate the accuracy are shown in Fig. 4.

It is observed that our introduced method yields good result in terms of accuracy. Human inspection may find difficulties to identify the dorsal and proximal-most point in blurred or dark images (row 5 and 7 of Fig. 4). However, our approach can solve all these problems. Again, to further specify the precision of our technique, we have tabulated the angles (AR & AL) and LRQ calculated using (3) by both our automatic system and manual procedure as reported in Table I. For calculating the error rate (E) of our method compared to manual, we used the following equation.

$$E = \frac{(Manual - Automatic) \times 100\%}{Manual} \tag{4}$$

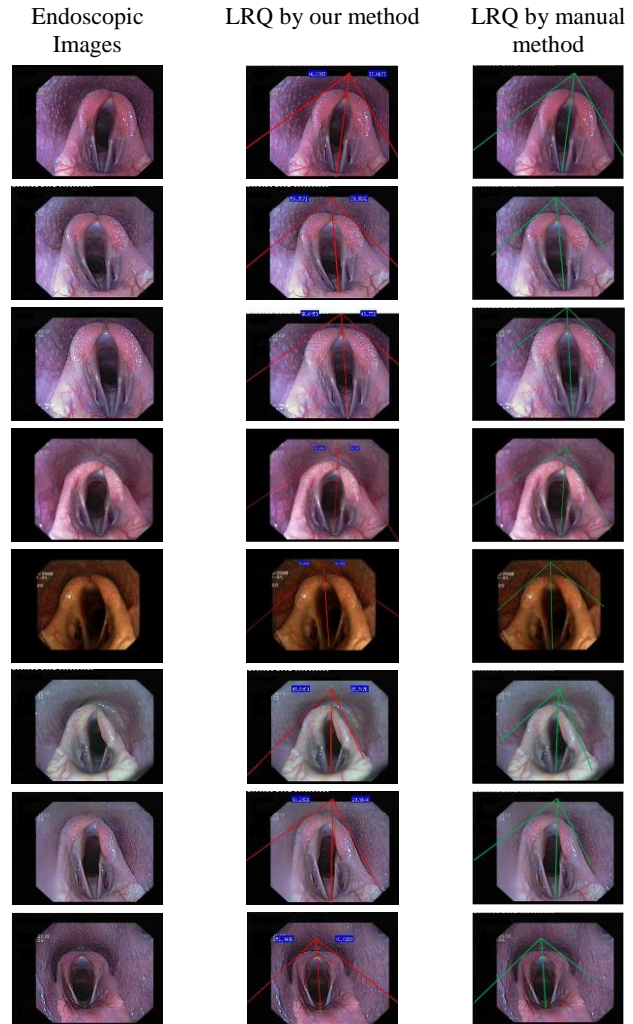


Figure 4. Sample results of the proposed method & ground truth (human measurement)

From Table I, it is clear to see that our approach can measure the angles and LRQ accurately without any further tuning and human intervention. Conversely, the success of the technique solely depends on the smoothness of segmentation algorithm and extraction of arytenoid cartilages and rima glottidis boundaries. Similarly, parallax error during human observation may cause large difference between proposed automatic method and manual one.

TABLE I. COMPARISON OF AR, AL AND LRQ MEASURED BY OUR APPROACH & HUMAN

No	Angles Calculated by Our Method		Angles Calculated by Manual Method		LRQ (our method)	LRQ (manual method)	Error Rate of LRQ (E)
	AL	AR	AL	AR			
1	46.69	37.01	45.50	37.50	0.79	0.82	3.66
2	55.39	39.36	54.00	39.50	0.71	0.73	2.74
3	56.04	42.73	55.50	44.00	0.76	0.79	3.80
4	53.40	35.71	53.00	35.00	0.67	0.66	1.52
5	51.81	51.15	50.00	49.00	0.99	0.98	1.02
6	43.94	25.74	45.00	25.50	0.59	0.57	3.51
7	53.23	28.56	52.00	29.00	0.54	0.56	3.57
8	51.04	40.02	49.00	48.00	0.96	0.98	2.04
Average error rate of LRQ							2.73

V. CONCLUSION

In this article, we have offered a fully automatic scheme to measure the angles between the vertical line and the right (AR) and the left (AL) tangential lines and calculate the right to left angle quotients (LRQ) to diagnose the laryngeal hemiplegia from endoscopic images. We applied this scheme to the sample endoscopic images of horse larynx and compared it with human estimation. Experimental results have shown that this approach is capable of computing AR, AL and LRQ without parameters adjustment just like a human observation with average error rate less than 3%. So, the proposed automatic and effective system will be a valuable tool for biomedical application in computer-aided clinical diagnosis of laryngeal hemiplegia.

REFERENCES

- [1] W. R. Cook, "The diagnosis of respiratory unsoundness in the horse," *The Veterinary Record*, vol. 77, pp. 516, 1965.
- [2] J. E. Brakenhoff, S. J. Holcombe, J. G. Hauptman, H. K. Smith, F. A. Nickels, and J. P. Caron, "The prevalence of laryngeal disease in a large population of competition draft horses," *Veterinary Surgery*, vol. 35, no. 6, pp. 579–583, 2006.
- [3] J. G. Lane, B. Bladon, D. R. M. Little, J. R. J. Naylor, and S. H. Franklin, "Dynamic obstructions of the equine upper respiratory tract-part 1: Observations during high-speed treadmill endoscopy of 600 thoroughbred racehorses," *Equine Veterinary Journal*, vol. 38, no. 5, pp. 393–399, 2006.
- [4] P. M. Dixon, B. C. McGorum, D. I. Railton, C. Hawe, W. H. Tremaine, K. Dacre, and J. McCann, "Long-term survey of laryngoplasty and ventriculocordectomy in an older, mixed-breed population of 200 horses-part 1: Maintenance of surgical arytenoid abduction and complications of surgery," *Equine Veterinary Journal*, vol. 35, no. 4, pp. 389–396, 2003.
- [5] N. Jansson, N. G. Ducharme, R. P. Hackett, and H. O. Mohammed, "An in vitro comparison of cordopexy, cordopexy and laryngoplasty, and laryngoplasty for treatment of equine laryngeal hemiplegia," *Veterinary Surgery*, vol. 29, no. 4, pp. 326–334, 2004.
- [6] J. D. Perkins, H. Meighan, Z. Windley, S. Troester, R. Piercy, and J. Schumacher, "In vitro effect of ventriculocordectomy before laryngoplasty on abduction of the equine arytenoid cartilage," *Veterinary Surgery*, vol. 40, no. 3, pp. 305–310, 2011.
- [7] H. Shah-Hosseini and R. Safabakhsh, "Automatic multilevel thresholding for image segmentation by the growing time adaptive self-organizing map," *IEEE Transactions on Pattern Analysis and Machine Intelligence*, vol. 24, no. 10, pp. 1388–1393, 2002.
- [8] S. A. Hojjatoleslami and J. Kittler, "Region growing: A new approach," *IEEE Transactions on Image Processing*, vol. 7, no. 7, pp. 1079–1084, 1998.
- [9] L. G. Roberts, *Machine Perception of Three-Dimensional Solids in Optical and Electro-Optical Information Processing*, J. Tippett, Ed., MIT Press, 1965, pp. 159–197.
- [10] R. O. Duda and P. E. Hart, *Pattern Classification and Scene Analysis*, New York: Wiley, 1973.
- [11] J. M. S. Prewitt, *Object Enhancement and Extraction*, New York: Academic Press, 1970, pp. 75–150.
- [12] J. Canny, "A computational approach to edge detection," *IEEE Transactions on Pattern Analysis and Machine Intelligence*, vol. 8, no. 6, pp. 679–698, June 1986.
- [13] A. Y. Yang, J. Wright, Y. Ma, and S. S. Sastry, "Unsupervised segmentation of natural images via lossy data compression," *Computer Vision and Image Understanding*, vol. 110, no. 2, pp. 212–225, 2008.
- [14] D. Comaniciu and P. Meer, "Mean shift: A robust approach toward feature space analysis," *IEEE Transactions on Pattern Analysis and Machine Intelligence*, vol. 24, no. 5, pp. 603–619, 2002.
- [15] P. F. Felzenszwalb and D. P. Huttenlocher, "Efficient graph-based image segmentation," *International Journal of Computer Vision*, vol. 59, no. 2, pp. 167–181, 2004.
- [16] P. Arbelaez, M. Maire, C. Fowlkes, and J. Malik, "Contour detection and hierarchical image segmentation," *IEEE Transactions on Pattern Analysis and Machine Intelligence*, vol. 33, no. 5, pp. 898–916, 2011.
- [17] The five-point conic. [Online]. Available: http://whistleralley.com/conics/conic_construction/5_pt_conic/
- [18] R. M. N. Sadat, Z. Sayeeda, M. M. Salehin, and N. Afrin, "A corner detection method using angle accumulation," in *Proc. 14th International Conf. on IEEE Computer and Information Technology*, Bangladesh, 2011, pp. 95–99.
- [19] P. D. Kovesi. (2000). Matlab and octave functions for computer vision and image processing. [Online]. Available: <http://www.csse.uwa.edu.au/~pk/Research/MatlabFns/#match>
- [20] C. Herholz and R. Straub, "Idiopathische hemiplegia laryngis (ihl) beim pferddiagnostik und aspekte der vererbung," *Swiss Vet*, vol. 11, pp. 56–58, 1995.



Md. M. Salehin is currently a PhD student at School of Computing & Mathematics, Charles Sturt University, Australia. His research area is in the field of image segmentation. He received his Bachelor of Science (B.Sc) degree in Computer Science and Engineering (CSE) from Rajshahi University of Engineering & Technology (RUET), Rajshahi, Bangladesh in 2006. His research interests are in the field of image segmentation, computer vision and pattern recognition.



Lihong, Zheng received her PhD degree in Computing Sciences from University of Technology, Sydney in 2008. She is currently senior lecturer at School of Computing and Mathematics, Charles Sturt University. Her previous research interest was on automation, robotics and artificial intelligence. Her current research interest is on computer vision, image processing, pattern recognition and machine learning. She had one patent and authored and co-authored more than forty papers in the field of artificial intelligence and image processing, machine learning and robotics.



Junbin Gao graduated from Huazhong University of Science and Technology (HUST), China in 1982 with B.Sc. degree in Computational Mathematics and obtained PhD from Dalian University of Technology, China in 1991. He is a Professor in Computing Science in the School of Computing and Mathematics at Charles Sturt University, Australia. He was a senior lecturer, a lecturer in Computer Science from 2001 to 2005 at University of New England, Australia. From 1982 to 2001 he was an associate lecturer, lecturer, associate professor and professor in Department of Mathematics at HUST. His main research interests include machine learning, data mining, bayesian learning and inference, and image analysis.